

Multiscale Methods for Wave Propagation in Heterogeneous Media Over Long Time

Björn Engquist, Henrik Holst, and Olof Runborg

Abstract Multiscale wave propagation problems are computationally costly to solve by traditional techniques because the smallest scales must be represented over a domain determined by the largest scales of the problem. We have developed and analyzed new numerical methods for multiscale wave propagation in the framework of the heterogeneous multiscale method (HMM). The numerical methods couple simulations on macro- and microscales for problems with rapidly oscillating coefficients. The complexity of the new method is significantly lower than that of traditional techniques with a computational cost that is essentially independent of the smallest scale, when computing solutions at a fixed time and accuracy. We show numerical examples of the HMM applied to long time integration of wave propagation problems in both periodic and non-periodic medium. In both cases our HMM accurately captures the dispersive effects that occur. We also give a stability proof for the HMM, when it is applied to long time wave propagation problems.

1 Introduction

We consider the initial boundary value problem for the scalar wave equation,

B. Engquist

Department of Mathematics and Institute for Computational Engineering and Sciences, The University of Texas at Austin, 1 University Station C1200, Austin TX 78712, U.S.A, e-mail: engquist@ices.utexas.edu

H. Holst

Department of Numerical Analysis, CSC, KTH, 100 44 Stockholm, Sweden, e-mail: holst@kth.se

Olof Runborg

Department of Numerical Analysis, CSC and Swedish e-Science Research Center (SeRC) KTH, 100 44 Stockholm, Sweden, e-mail: olofr@nada.kth.se

$$\begin{cases} u_{tt}^\varepsilon - \nabla \cdot A^\varepsilon \nabla u^\varepsilon = 0, & \Omega \times [0, T], \\ u^\varepsilon(x, 0) = f(x), \quad u_t^\varepsilon(x, 0) = g(x), & \forall x \in \Omega, \end{cases} \quad (1)$$

on a smooth domain $\Omega \subset \mathbb{R}^N$ where $A^\varepsilon(x)$ is a symmetric, uniformly positive definite matrix. The expression $\nabla \cdot A^\varepsilon \nabla u^\varepsilon$ should be interpreted as $\nabla \cdot (A^\varepsilon \nabla u^\varepsilon)$. For simplicity we assume that Ω is a hypercube in \mathbb{R}^N with periodic boundary conditions. We assume that A^ε has oscillations on a scale proportional to $\varepsilon \ll 1$. The solution of (1) will then be a sum of two parts: one coarse scale (macroscale) part, which is independent of ε , and an oscillatory (microscale) part which is highly oscillating in both time and spatial directions on the scale ε . These kinds of multiscale problems are typically very computationally costly to solve by traditional numerical techniques. The smallest scale must be well represented over a domain which is determined by the largest scale of interest. However most often one is only interested in the coarse scale part of the solution. The goal of our research here is to find an efficient way to compute it.

Recently, new frameworks for numerical multiscale methods have been proposed. These include the heterogeneous multiscale method (HMM) [5] and the equation free approach [14]. They couple simulations on macro- and microscales to compute the coarse scale solution efficiently. The HMM framework has been applied to a number of multiscale problems, for example, ODEs with multiple time scales [12], elliptic and parabolic equations with multiscale coefficients [7, 17, 1], kinetic schemes [6] and large scale MD simulations of gas dynamics [15]. In this paper we use HMM for the wave equation. Our method builds on [10] where we described a HMM multiscale method which captured the coarse scale behavior of (1) for finite time. See also [2]. The main aim here is to show that the HMM methodology in [10] works also for long time, where new macroscale phenomena occurs.

As an inspiration for designing our HMM we first consider the classical homogenization theory, in which the coarse scale properties of partial differential equations with rapidly oscillating coefficients, like (1), can be analyzed. For example, in the setting of composite materials consisting of two or more mixed constituents (i.e., thin laminated layers that are ε -periodic), homogenization theory gives the effective properties of the composite. It is an interesting remark that the effective properties often are different than the average of the individual constituents that makes up the composite [4]. The main homogenization result is that, under certain conditions, when the period of the coefficients in the PDE goes to zero, the solution approaches the solution to another PDE which has no oscillatory (microscale) part. This *homogenized* PDE is very useful from a numerical perspective. It gives a coarse scale solution and the coefficients in the PDE have no ε -dependency. That means that the homogenized PDE is inexpensive to solve with standard numerical methods. At the same time the solution is a good approximation of the coarse scale (macroscopic) part of the original equation. For our multiscale problem (1) with $A^\varepsilon(x) = A(x, x/\varepsilon)$ and where $A(x, y)$ is periodic in y , the homogenized PDE is of the form,

$$\begin{cases} \bar{u}_{tt} - \nabla \cdot \bar{A} \nabla \bar{u} = 0, & \Omega \times [0, T], \\ \bar{u}(x, 0) = f(x), \quad \bar{u}_t(x, 0) = g(x), & \forall x \in \Omega, \end{cases} \quad (2)$$

where $\bar{A}(x)$ is the homogenized or effective coefficient. We refer to [3, 18, 4, 13, 16, 11] for more details about homogenization.

Homogenization gives the limit PDE as $\varepsilon \rightarrow 0$ for a constant T (independent of ε). The use of classical homogenization is limited by the fact that it does not describe the dispersive effects in (1) that occur when T becomes very large. Santosa and Symes [20] developed effective medium equations for wave propagation problems with $T = \mathcal{O}(\varepsilon^{-2})$. In the one-dimensional case, when $A^\varepsilon(x) = A(x/\varepsilon)$ and A periodic, this equation will be of the form

$$\tilde{u}_{tt} - \bar{A} \tilde{u}_{xx} - \beta \varepsilon^2 \tilde{u}_{xxxx} = 0,$$

where \bar{A} is the same coefficient as in (2) and β is a functional of A . The effective medium solution \tilde{u} can be used as an approximation for longer time than the homogenized solution \bar{u} with an error of the form $\mathcal{O}(\varepsilon) + \mathcal{O}(\varepsilon^3 t)$. See [20] for further details about this model.

We will now briefly describe the typical setting of HMM for multiscale problems and how it can be applied to (1). We assume that there exists two models, a micro model $h(u^\varepsilon, d^\varepsilon) = 0$ describing the full problem, where u^ε is the quantity of interest and d^ε is the problem data (i.e. initial conditions, boundary conditions, ...), and a coarse macro model $H(u, d) = 0$, with solution u and data d . The micro model is accurate but is expensive to compute by traditional methods. In our case this model is (1). The macro model gives a coarse scale solution u , assumed to be a good approximation of the microscale solution u^ε and is less expensive to compute. The model is however incomplete in some sense and requires additional data. In our case we use

$$u_{tt} - \nabla \cdot F = 0,$$

with the flux F unknown. This is inspired by the form of the homogenized equation (2). A key idea in the HMM is to provide the missing data in the macro model using local solutions of the micro model. Here (1) is solved locally on a small domain with size proportional to ε and F is given as an average of the resulting microscopic flux $A^\varepsilon \nabla u^\varepsilon$. The initial data and boundary conditions (d^ε) for this computation is constrained by the macroscale solution u .

It should be noted that even if our numerical methods use ideas from homogenization theory they do not solve any effective (e.g. homogenization or effective medium) equation directly. The goal is to develop computational techniques that can be used when there is no fully known macroscopic PDE.

The article is organized as follows: In Sect. 2 we describe our HMM for the wave equation for finite time. In Sect. 3 we describe the modifications made to our HMM for the long time problem and in Sect. 3.4 we describe the theory behind the long time problem. We also treat problems which do not fit the theory. In Sect. 3.3 where we solve a non-periodic problem for long time. We end this paper with our conclusions in the closing Sect. 4.

2 HMM for the Wave Equation and Finite Time

We continue here with the description of our HMM method for the wave equation (1) over finite time. By finite time we mean that the final time T is independent of ε . In the next section we will consider cases where $T = T(\varepsilon) \rightarrow \infty$ as $\varepsilon \rightarrow 0$.

The HMM method we suggest here is described in three separate steps. We follow the same strategy as in [1] for parabolic equations and in [19] for the one-dimensional advection equation. See [8], [10] and [2] for additional details and proofs. In step one we give the macroscopic PDE (i.e. the form $H(u, d) = 0$) and a corresponding numerical discretization. In step two we describe the microscale problem (microproblem). The initial data for the microproblem is based on local macroscopic data. Finally, in step three we describe how we approximate F from the computed microproblem by taking a weighted average of its solution.

We will assume that the domain $\Omega = Y \subset \mathbb{R}^d$ is a hypercube such that our microscopic PDE is of the form,

$$\begin{cases} u_{tt}^\varepsilon - \nabla \cdot A^\varepsilon \nabla u^\varepsilon = 0, & Y \times [0, T], \\ u^\varepsilon(x, 0) = f(x), \quad u_t^\varepsilon(x, 0) = g(x), & \forall x \in Y. \end{cases} \quad (3)$$

and $u^\varepsilon(x, t)$ is Y -periodic in x .

Step 1: Macro model and discretization

We suppose there exists a macroscale PDE of the form,

$$\begin{cases} u_{tt} - \nabla \cdot F(x, u, \nabla u, \dots) = 0, & Y \times [0, T], \\ u(x, 0) = f(x), \quad u_t(x, 0) = g(x), & \forall x \in Y, \\ u \text{ is } Y\text{-periodic,} \end{cases} \quad (4)$$

where F is a function of x, u and higher derivatives of u . We will use this assumption throughout the whole paper. Another assumption is that $u \approx u^\varepsilon$ when ε is small. In the method we suppose that $F = F(x, \nabla u)$. In the clean homogenization case we would have $F = \bar{A} \nabla u$, but we will not assume knowledge of a homogenized equation.

We discretize (4) using central differences with time step K and spatial grid size H in all directions,

$$\begin{cases} U_m^{n+1} = 2U_m^n - U_m^{n-1} + \frac{K^2}{H} \sum_{i=1}^d \left(e_i^T F_{m+\frac{1}{2}e_i}^n - e_i^T F_{m-\frac{1}{2}e_i}^n \right), \\ F_{m-\frac{1}{2}e_k}^n = F(x_{m-\frac{1}{2}e_k}, P_{m-\frac{1}{2}e_k}^n), \quad k = 1, \dots, d, \\ \text{(Note that } F_{m-\frac{1}{2}e_k}^n \text{ is a vector.)} \end{cases} \quad (5)$$

where $F_{m-\frac{1}{2}e_k}^n$ is F evaluated at point $x_{m-\frac{1}{2}e_k}$. The quantity $P_{m-\frac{1}{2}e_k}^n$ approximates ∇u in the point $x_{m-\frac{1}{2}e_k}$.

Step 2: Micro problem

The evaluation of $F_{m-\frac{1}{2}e_k}^n$ in each grid point is done by solving a micro problem to evaluate the flux values in (5). Given the parameters $x_{m-\frac{1}{2}e_k}$ and $P_{m-\frac{1}{2}e_k}^n$, we solve

$$\begin{cases} u_{tt}^\varepsilon - \nabla \cdot A^\varepsilon \nabla u^\varepsilon = 0, & Y^\varepsilon \times [-\tau, \tau], \\ u^\varepsilon(x, 0) = (P_{m-\frac{1}{2}e_k}^n) \cdot x, \quad u_t^\varepsilon(x, 0) = 0, & \forall x \in Y^\varepsilon, \\ u^\varepsilon - u^\varepsilon(x, 0) \text{ is } Y^\varepsilon\text{-periodic,} \end{cases} \quad (6)$$

where $x - x_{m-\frac{1}{2}e_k} \mapsto x$ and $t - t_n \mapsto t$. The initial data $u^\varepsilon(x, 0)$ is a linear polynomial approximating the macroscopic solution locally, modulo a constant term; since we only consider the derivative of u^ε when computing F below, the constant term does not affect the result.

We keep the sides of the micro box Y^ε of order ε . We note that the solution u^ε is an even function with respect to t (i.e. $u^\varepsilon(x, -t) = u^\varepsilon(x, t)$) due to the initial condition $u_t^\varepsilon(x, 0) = 0$.

Step 3: Reconstruction step

After we have solved for u^ε for all $Y^\varepsilon \times [-\tau, \tau]$ we approximate $F_{m-\frac{1}{2}e_k}^n$ by a weighted average of $f^\varepsilon = A^\varepsilon \nabla u^\varepsilon$ over $[-\eta, \eta]^d \times [-\tau, \tau]$ where $[-\eta, \eta]^d \subset Y^\varepsilon$. We choose η, τ sufficiently small so that information will not propagate into the region $[-\eta, \eta]^d$ from the boundary of the micro box Y^ε in $[-\tau, \tau]$ time. More precisely, we consider averaging kernels K described in [12]: We let $\mathbb{K}^{p,q}$ denote the kernel space of functions K such that $K \in C_c^q(\mathbb{R})$ with $\text{supp } K = [-1, 1]$ and

$$\int K(t)t^r dt = \begin{cases} 1, & r = 0; \\ 0, & 1 \leq r \leq p. \end{cases}$$

Furthermore we will denote K_η as a scaling $K_\eta(x) := \eta^{-1}K(x/\eta)$ with compact support in $[-\eta, \eta]$. We then approximate

$$F_{m-\frac{1}{2}e_k}^n \approx \tilde{F}(x_{m-\frac{1}{2}e_k}, P_{m-\frac{1}{2}e_k}^n) = \iint K_\tau(t) K_\eta(x_1) \cdots K_\eta(x_d) f_k^\varepsilon(x, t) dx dt, \quad (7)$$

where $f^\varepsilon(x, t) = A^\varepsilon(x + x_{m-\frac{1}{2}e_k}) \nabla u^\varepsilon(x, t)$.

We proved in [10] that if we apply the HMM to the problem (1) with $A^\varepsilon(x) = A(x/\varepsilon)$ where A is a Y -periodic symmetric positive matrix the HMM generates re-

sults close to a direct discretization of the homogenized equation (2). In particular, we showed that

$$\tilde{F}(x, y) = F(x, y) + \mathcal{O}\left(\left(\frac{\varepsilon}{\eta}\right)^{q+2}\right).$$

The function \tilde{F} and F are defined in (7) and (4) respectively and we note that here $F(x, y) = \bar{A}y$. The integer q depends on the smoothness of the kernel used to compute the weighted average of f^ε in (7).

Theorem 1. *Let $\tilde{F}(x_0, y)$ be defined by (7) where u^ε solves the micro problem (6) exactly, $A^\varepsilon(x) = A(x/\varepsilon)$ and A is Y -periodic and C^∞ . Moreover suppose $K \in \mathbb{K}^{p,q}$, f and g are C^∞ and $\tau = \eta$. Then for $y \neq 0$ and any dimension,*

$$\frac{1}{\|y\|} |\tilde{F}(x_0, y) - F(x_0, y)| \leq C \left(\frac{\varepsilon}{\eta}\right)^{q+2},$$

where C is independent of ε and η . Furthermore, for the numerical approximation given in (5) in one dimension, with $H = n\varepsilon$ for some integer n and smooth initial data, we have the error estimate

$$|U_m^n - \bar{u}(x_m, t_n)| \leq C(T) \left(H^2 + (\varepsilon/\eta)^{q+2}\right), \quad 0 \leq t_n \leq T,$$

where \bar{u} is the homogenized solution to (2).

Remark 1. The weighted integrals above are computed numerically with a simple trapezoidal rule in time and a midpoint rule in space.

Remark 2. In our implementation, the micro problem (6) is solved by the same numerical scheme as the macro problem (5).

Remark 3. We assume that our scheme for the microproblem can have a constant number of grid points per ε to maintain a fixed accuracy. This implies that a direct solver for (3) on the full domain has a cost of order $\varepsilon^{-(d+1)}$. The total cost for on-the-fly HMM is of the form (cost of micro problem) $\times M_d$ where

$$M_d \sim \frac{1}{K} \cdot \frac{1}{H^d}$$

is the number of micro problems needed to be solved. The macro PDE can be discretized independently of ε therefore M_d does not depend on ε . If we choose η and τ proportional to ε the cost of a single micro problem $(\tau/\varepsilon) \times (\eta/\varepsilon)^d$ is also independent of ε . In conclusion our HMM method has a computational cost independent of ε .

Remark 4. We can to reduce the computational cost of the HMM process even further if the function \tilde{F} in (7) is linear in some of its arguments. We can then apply the HMM process to a smaller number of micro problems and form linear combinations of those for any given \tilde{F} computation. If \tilde{F} depends on u or t it might not be beneficial to precompute \tilde{F} this way. See [10] for further details.

Remark 5. The macro scheme suggested here is embarrassingly parallel in space. This fact has been exploited by the authors in a Fortran 90 code with MPI parallelization. We think that it would be possible to implement the same algorithm in a general purpose GPU environment and see a good utilization of the hardware.

2.1 One Numerical Example

We consider the one-dimensional problem of the form (1),

$$\begin{cases} u_{tt}^\varepsilon - \partial_x A^\varepsilon u_x = 0, & [0, 1] \times [0, 1], \\ u^\varepsilon(x, 0) = \exp(-100x^2) + \exp(-100(1-x)^2), & u_t(x, 0) = 0, \quad x \in [0, 1], \\ u^\varepsilon \text{ is 1-periodic,} \end{cases} \tag{8}$$

for $A^\varepsilon(x) = A(x/\varepsilon)$ where $A(y) = 1.1 + \sin 2\pi y$. The homogenized equation will then have the form (2) with $\bar{A} = \left(\int_0^1 \frac{1}{A(s)} ds\right)^{-1} = \sqrt{0.21}$. Since we have periodic boundary conditions, the solution to the homogenized equation will be periodic in time with period $1/\sqrt{\bar{A}} \approx 1.47722$. We show the solution after one full period. The numerical parameters are $H = 1.0 \cdot 10^{-2}, K = 1.0 \cdot 10^{-3}, \eta = \tau = 0.05, h = 1.5 \cdot 10^{-4}$ and $k = 7.8 \cdot 10^{-5}$. We take $\varepsilon = 0.01$. See Fig. 1 for a plot of the result. We refer to [10] for further examples where HMM is applied to other finite time problems.

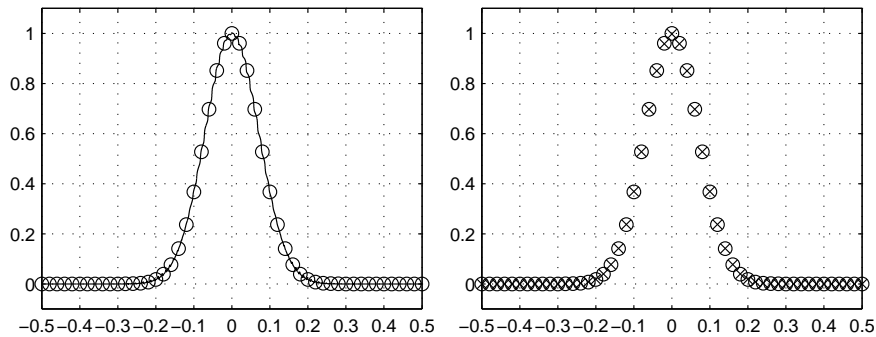


Fig. 1 Results from solving (8) with a finite difference method, DNS (direct numerical simulation), and the corresponding homogenized equation with highly accurate spectral method (circles), compared to our HMM method (crosses). The fast $\mathcal{O}(\varepsilon)$ oscillations are visible as small fluctuations in the DNS computation.

3 HMM for the Wave Equation over Long Time

Classical homogenization deals with constant T (i.e. independent of ε) and finds the limiting PDE as $\varepsilon \rightarrow 0$. We demonstrated in the previous section that our HMM captures the same solution as homogenization (when applicable). In this section we will investigate how our HMM method, after some minor changes, handles the case when $T = \mathcal{O}(\varepsilon^{-2})$. The microscopic variations in the medium introduces dispersive effects in the macroscopic behavior of the solution, after long time. Our goal is to show that our HMM method can capture the dispersion with less computational cost than just resolving the full equation.

Let us illustrate the dispersive effects by a numerical example. We consider the same one-dimensional example (8) as above, but solve it for a long time $T = \mathcal{O}(\varepsilon^{-2})$. We compute the solutions after 1, 10 and 100 periods (≈ 1.47722) of the homogenized equation. We see in Fig. 2 that after 100 periods there is an $\mathcal{O}(1)$ error between the true solution u^ε and the homogenized solution \bar{u} which thus fails to capture the dispersive behavior of the solution after long time.

3.1 The HMM Algorithm for Long Time

We must make a few minor modifications to our original HMM algorithm in Sect. 2 in order to capture the dispersive effects seen in Fig. 2. We will now describe those changes. They can all be seen as modifications to increase accuracy.

Step 1: Macro model and discretization

We assume the macroscopic PDE still is of the form $u_{tt} - \nabla \cdot F = 0$ where F depends on u and its derivatives but we will use a higher order scheme instead of (5). The scheme below has better dispersive properties and hence allow us to better avoid some of the numerical dispersion,

$$U_m^{n+1} = 2U_m^n - U_m^{n-1} + \frac{K^2}{24H} \left(-F_{m+3/2}^n + 27F_{m+1/2}^n - 27F_{m-1/2}^n + F_{m-3/2}^n \right),$$

where $F_{m-\frac{1}{2}}^n$ is computed in the same fashion as before in step 2 and 3, defined below.

Step 2: Micro problem

The initial data for the micro problem for finite time (6) is modified to a cubic polynomial $Q(x)$,

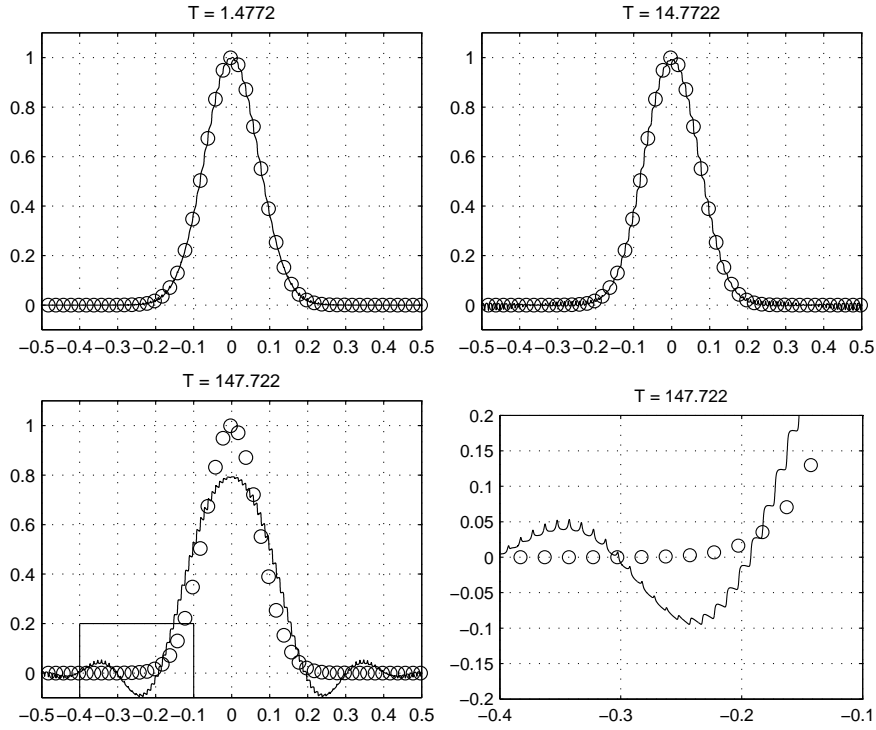


Fig. 2 Finite difference computation of (8) at $T = 1.47722$, $T = 14.7722$ and $T = 147.722$ (1, 10 and 100 periods of the homogenized solution) and the corresponding homogenized solution (circles). As we can see the homogenized solution does not capture the dispersive effects that occur.

$$\begin{cases} u_{tt}^\varepsilon - \partial_x A^\varepsilon u_x^\varepsilon = 0, & Y^\varepsilon \times [-\tau, \tau], \\ u^\varepsilon(x, 0) = Q(x), \quad u_t^\varepsilon(x, 0) = 0, & \forall x \in Y^\varepsilon, \\ u^\varepsilon \text{ is } Y^\varepsilon\text{-periodic,} \end{cases}$$

The state of the macroscopic solution is then more accurately represented by the initial data. The cubic polynomial is chosen as follows when computing the flux $F_{m+1/2}$. Let $\tilde{Q}(x)$ interpolate the macroscopic solution in the four grid points surrounding $x_{m+1/2}$. Then use $Q(x) = \tilde{Q}(x) - \gamma \varepsilon^2 \tilde{Q}''(x)$. The small correction is needed to get an initialization that is consistent with the macroscopic data $\tilde{Q}(x)$ to high order in ε . The factor γ can be determined numerically, see Sect. 3.4.

Step 3: Reconstruction step

The average is computed as before but we need to use a sufficiently accurate kernel K and take the average over a bit larger box, i.e. larger τ and η with respect to ε such that $\tau, \eta \sim \varepsilon^{1-\alpha}$ with $\alpha > 0$. We will delay the discussion about α until Sect. 3.4.

3.2 A Long Time Computation with HMM

We solved the problem (8) using the HMM algorithm, with the improvements described above. As before we computed the solution after 1, 10 and 100 periods of the homogenized equation. In Fig. 3 we see that the HMM algorithm is able to accurately approximate the solution also after long time, and thus captures the correct dispersive effects.

The HMM solver uses $H = 5.7 \cdot 10^{-3}$, $K = 5.7 \cdot 10^{-4}$ and a kernel with $\tau = \eta = 0.5$ from $\mathbb{K}^{9,9}$ which is a 9 times continuously differentiable compact function with support $[-1, 1]$. The micro solver and the DNS solver uses $h = 7.8 \cdot 10^{-5}$ and $k = 3.9 \cdot 10^{-5}$. We take $\varepsilon = 0.01$. Note that since the integration time T is very long we need to take H rather small to avoid dispersion errors in the macroscopic integration.

3.3 Non-Periodic Material

We consider the problem (1) with a function A^ε which is not periodic on the microscale,

$$A^\varepsilon(x) = A(rx/\varepsilon, x/\varepsilon), \quad \text{and} \quad A(y_1, y_2) = 1.1 + \frac{1}{2} (\sin 2\pi y_1 + \sin 2\pi y_2),$$

where r is an irrational number. We take $r = \sqrt{2}$. To be precise we take $r = 1.41$ and $\varepsilon = 0.01$ to ensure A^ε is periodic on the macroscopic scale. There is no cell problem for this A^ε but it is well known that there is a homogenized equation of the form (2) with $\bar{A} = (\int_0^1 \frac{1}{A^\varepsilon(x)} dx)^{-1} = 0.744157$ and thus the period length is $1/\sqrt{\bar{A}} = 1.15922$. The initial data is $u(x, 0) = \exp(-100x^2) + \exp(-100(1-x)^2)$ and $u_t(x, 0) = 0$.

We compare our HMM-results with an accurate DNS computation after 10 and 100 periods. We use $\eta = \tau = 0.5$ and a kernel $K \in \mathbb{K}^{9,9}$. The numerical parameters are $H = 5.7 \cdot 10^{-3}$, $K = 5.7 \cdot 10^{-4}$, $h = 7.8 \cdot 10^{-5}$ and $k = 3.9 \cdot 10^{-5}$. See Fig. 3.3.

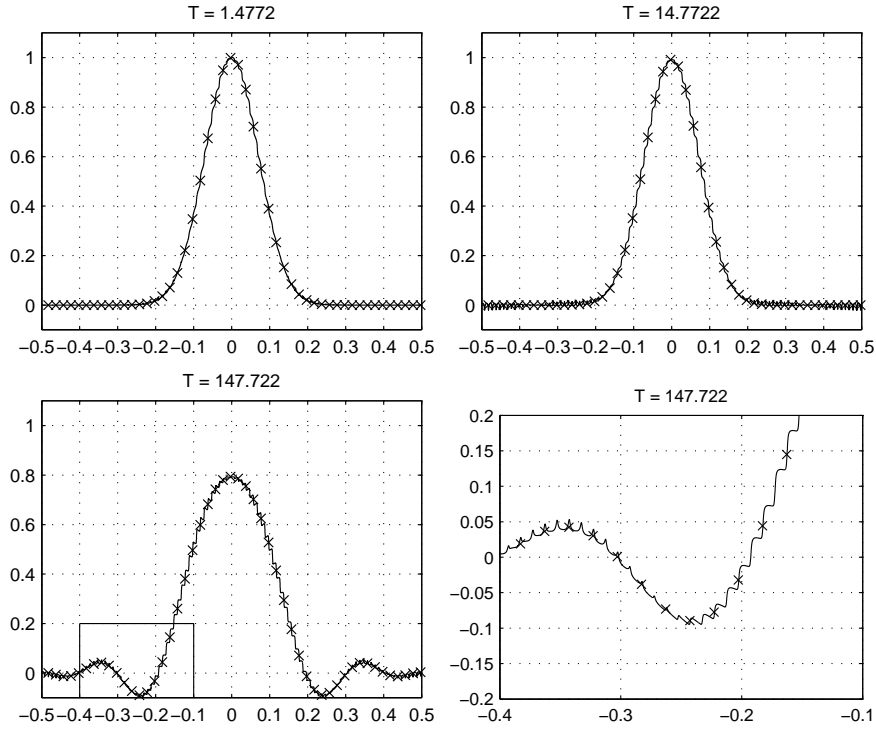


Fig. 3 A longtime DNS simulation (thin line) compared to an HMM solution (crosses) at $T = 1.47722$, $T = 14.7722$ and $T = 147.722$ (1, 10 and 100 periods of the homogenized solution) for the example in Sect. 3.2. As we can see, the HMM method gives good agreement with the true solution also after long time.

3.4 Theory

We will now give a motivation to why our HMM method works also for long time. In classical homogenization theory the homogenized solution \bar{u} satisfies a homogenized PDE. The solution u is a good approximation to the true solution u^ε such that $\|u^\varepsilon(t, \cdot) - \bar{u}(t, \cdot)\|_{L^2} = \mathcal{O}(\varepsilon)$, upto a fixed time T independent of ε . Santosa and Symes derived an equation for a similar quantity \tilde{u} which approximates u^ε with an error of the form $\mathcal{O}(\varepsilon) + \mathcal{O}(\varepsilon^3 t)$ for $T = \mathcal{O}(\varepsilon^{-2})$. We will now describe some of the theory presented in [20]. The theory thus extends the effective model (2) with additional terms, from $T = \mathcal{O}(1)$ up to time $T = \mathcal{O}(\varepsilon^{-2})$.

Let us first give some definitions. Let ω_m^2 and ψ_m be the eigenvalues and eigenfunctions of the shifted cell (eigenvalue) problem [3, pp. 614],

$$\begin{cases} -(\partial_y + ik)A(y)(\partial_y + ik)\psi(y, k) = \omega^2(k)\psi(y, k), & Y \times Y, \\ \psi(y, k) \text{ is } Y\text{-periodic in } y, \end{cases}$$

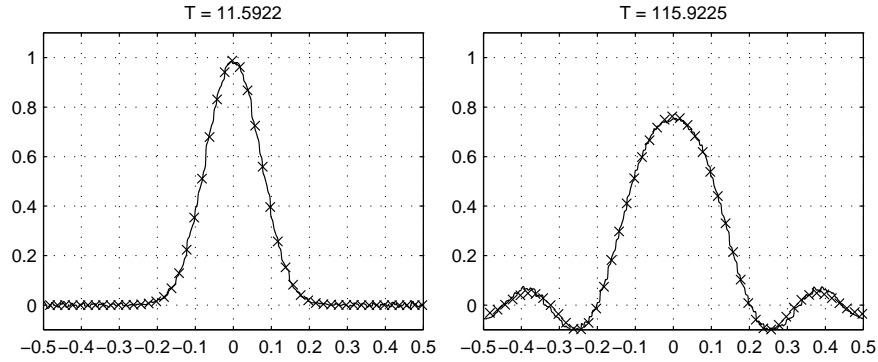


Fig. 4 Numerical result from the example in Sect. 3.3. A longtime DNS simulation (thin line) compared to an HMM solution (crosses) at $T = 11.5922$ and $T = 115.922$ (10 and 100 periods of the homogenized solution). The dispersion effects appearing after long time is captured by our HMM method.

where $Y = [0, 1]^d$ and $k \in \mathbb{R}^d$. Let $v_m(x, k)$ be the scaled Bloch-waves,

$$v_m(x, k) = \Psi_m(x/\varepsilon, \varepsilon k) \exp(ik \cdot x),$$

which satisfies

$$-\partial_x \left(a \left(\frac{x}{\varepsilon} \right) \partial_x v_m \right) = \frac{1}{\varepsilon^2} \omega_m^2(\varepsilon k) v_m.$$

The functions U_m and \hat{f}_m are defined as the projection of u^ε and f on v_m ,

$$U_m(k, t) = \int u^\varepsilon(x, t) v_m^*(x, k) dx, \quad \hat{f}_m(k) = \int f(x) v_m^*(x, k) dx.$$

Throughout this section we assume that the initial data $f(x)$ is a bandlimited function. The following theorem from [20] then states that if we expand the solution to the wave equation in the basis given by $\{v_m\}$, the terms with $m \geq 1$ are bounded by $\mathcal{O}(\varepsilon)$ uniformly in time.

Theorem 2. *Suppose u^ε solves (1) with $g = 0$ and expand*

$$u^\varepsilon(x, t) = \int_{Y/\varepsilon} U_0(k, t) v_0(x, k) dk + \sum_{m=1}^{\infty} \int_{Y/\varepsilon} U_m(k, t) v_m(x, k) dk. \quad (9)$$

Then

$$\int_{\mathbb{R}^3} \left| \sum_{m=1}^{\infty} \int_{Y/\varepsilon} U_m(k, t) v_m(x, k) dk \right|^2 dx \leq C \varepsilon^2.$$

Here C is independent of ε and t but depends on the H^2 -norm of the initial data f and the L^∞ -norm of a and ∇a .

See [20] for proof.

We denote the first term in (9) by u_0 and note that $\hat{f}_0(k)$ has compact support if $f(x)$ is band limited, see [20]. Then, for some fixed L ,

$$\begin{aligned} u_0(x,t) &= \frac{1}{2} \int_{Y/\varepsilon} \hat{f}_0(k) v_0(x,k) \exp(\pm i\omega_0(\varepsilon k)t/\varepsilon) dk \\ &= \frac{1}{2} \int_{-L}^L \hat{f}_0(k) \psi_0(x/\varepsilon, \varepsilon k) \exp(ikx + i\omega_0(\varepsilon k)t/\varepsilon) dk. \end{aligned}$$

We now Taylor expand ψ_0 in the second argument and use the fact that $\psi_0(x,0) \equiv 1$. This gives

$$\begin{aligned} u_0(x,t) &= \frac{1}{2} \int_{-L}^L \hat{f}_0(k) (\psi_0(x/\varepsilon, 0) + \mathcal{O}(\varepsilon k)) \exp(ikx + i\omega_0(\varepsilon k)t/\varepsilon) dk \\ &= \frac{1}{2} \int_{-L}^L \hat{f}_0(k) \exp(ikx + i\omega_0(\varepsilon k)t/\varepsilon) dk + \mathcal{O}(\varepsilon). \end{aligned}$$

Next we Taylor expand $\omega_0(\varepsilon k)$ around $k = 0$,

$$\begin{aligned} \omega_0(\varepsilon k) &= \omega_0(0) + \varepsilon k \omega_0'(0) + \frac{\varepsilon^2 k^2}{2!} \omega_0''(0) + \frac{\varepsilon^3 k^3}{3!} \omega_0^{(3)}(0) + \mathcal{O}(\varepsilon^4 k^4) \\ &=: \tilde{\omega}_0(\varepsilon k) + \mathcal{O}(\varepsilon^4 k^4), \end{aligned}$$

and plug this expansion into the expression for u_0 ,

$$\begin{aligned} u_0(x,t) &= \frac{1}{2} \int_{-L}^L \hat{f}_0(k) \exp(ikx + i[\tilde{\omega}_0(\varepsilon k) + \mathcal{O}(\varepsilon^4 k^4)]t/\varepsilon) dk + \mathcal{O}(\varepsilon) \\ &= \frac{1}{2} \int_{-L}^L \hat{f}_0(k) \exp(ikx + i\tilde{\omega}_0(\varepsilon k)t/\varepsilon) dk + \mathcal{O}(\varepsilon^3 t) + \mathcal{O}(\varepsilon) \\ &=: \tilde{u}_0(x,t) + \mathcal{O}(\varepsilon^3 t) + \mathcal{O}(\varepsilon). \end{aligned}$$

Let us now differentiate the leading term $\tilde{u}_0(x,t)$ twice with respect to t ,

$$\partial_{tt} \tilde{u}_0(x,t) = \frac{1}{2} \int_{-L}^L -\frac{1}{\varepsilon^2} (\tilde{\omega}_0(\varepsilon k))^2 \hat{f}_0(k) \exp(ikx + i\tilde{\omega}_0(\varepsilon k)t/\varepsilon) dk$$

and upon expanding the square of $\tilde{\omega}_0$ under the integral we obtain

$$\begin{aligned}
\partial_{tt}\tilde{u}_0(x,t) = & -\frac{1}{2}\int_{-L}^L \left[\varepsilon^{-2}\omega_0(0)^2 2\varepsilon^{-1}k\omega_0(0)\omega_0'(0) \right. \\
& + \frac{1}{2}k^2(2\omega_0(0)\omega_0''(0) + 2(\omega_0'(0))^2) \\
& + \frac{1}{6}\varepsilon k^3(2\omega_0(0)\omega_0^{(3)}(0) + 6\omega_0'(0)\omega_0''(0)) \\
& + \frac{1}{24}\varepsilon^2 k^4(8\omega_0'(0)\omega_0^{(3)}(0) + 6(\omega_0''(0))^2) \\
& \left. + \frac{1}{6}\varepsilon^3 k^5(\omega_0''(0)\omega_0^{(3)}(0)) + \frac{1}{36}\varepsilon^4 k^6(\omega_0^{(3)}(0))^2 \right] \times \\
& \hat{f}_0(k) \exp(ikx + i\tilde{\omega}_0(\varepsilon k)t/\varepsilon) dk.
\end{aligned}$$

We now use the facts that $\omega_0(0) = 0$ and that by symmetry all odd derivatives of $\omega_0^2(k)$ are zero when evaluated at $k = 0$. Then the expression for $\partial_{tt}\tilde{u}_0$ simplifies to

$$\begin{aligned}
\partial_{tt}\tilde{u}_0(x,t) = & -\frac{1}{2!}\int_{-L}^L \left[\frac{1}{2}k^2 \frac{\partial^2 \omega_0^2(k)}{\partial k^2} \Big|_{k=0} + \frac{1}{4!}\varepsilon^2 k^4 \frac{\partial^4 \omega_0^2(k)}{\partial k^4} \Big|_{k=0} \right. \\
& \left. + \varepsilon^3 k^5 R_1 + \varepsilon^4 k^6 R_2 \right] \hat{f}_0(k) \exp(ikx + i\tilde{\omega}_0(\varepsilon k)t/\varepsilon) dk \\
= & \frac{1}{2!} \frac{\partial^2 \omega_0^2(k)}{\partial k^2} \Big|_{k=0} \partial_{xx}\tilde{u}_0(x,t) - \varepsilon^2 \frac{1}{4!} \frac{\partial^4 \omega_0^2(k)}{\partial k^4} \Big|_{k=0} \partial_{xxxx}\tilde{u}_0(x,t) \\
& - i\varepsilon^3 R_1 \partial_{xxxx}\tilde{u}_0(x,t) - \varepsilon^4 R_2 \partial_{xxxx}\tilde{u}_0(x,t), \tag{10}
\end{aligned}$$

where R_1 and R_2 are some real numbers. This is approximated in [20] with the PDE

$$\tilde{u}_{tt} = \bar{A}\tilde{u}_{xx} + \beta\varepsilon^2\tilde{u}_{xxxx}, \tag{11}$$

where

$$\bar{A} = \frac{1}{2!} \frac{\partial^2 \omega_0^2}{\partial k^2} \Big|_{k=0}, \quad \beta = -\frac{1}{4!} \frac{\partial^4 \omega_0^2}{\partial k^4} \Big|_{k=0}.$$

The remaining $m \geq 1$ terms in (9) are as we said uniformly bounded by $\mathcal{O}(\varepsilon)$ in L_2 -norm, so that we can use $\tilde{u} \approx \tilde{u}_0$ as an $\mathcal{O}(\varepsilon)$ approximation up to the time $t = \mathcal{O}(\varepsilon^{-2})$. We present a final comparison based on the example (8) in Fig. 5

We arrive at three conclusions from the analysis above:

1. The long time effective equation (11) is of the form

$$\tilde{u}_{tt} - \partial_x F = 0, \quad F = \bar{A}\tilde{u}_x + \beta\varepsilon^2\tilde{u}_{xxx}.$$

This fits into the assumed form of our macroscale PDE in (4) and we do not need to change the HMM algorithm to reflect a different macro model.

2. The flux F contains a third derivative of the macroscopic solution. In order to pass this information on to the micro simulation, the initial data must be at least a third order polynomial. This explains why the linear initial data used in the finite time HMM is not enough.

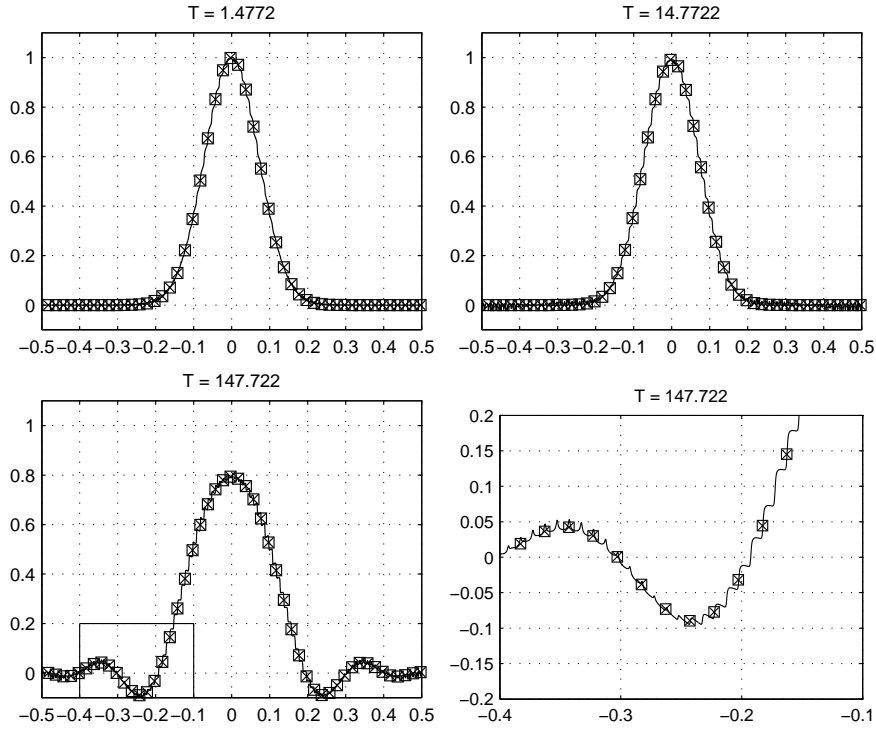


Fig. 5 Numerical result from example in Sect. 3.2: a long time DNS computation (thin line) compared to a direct discretization of the long time effective equation (11) with a coarse grid (squares) and our HMM method (crosses).

- Since we need to accurately represent also the second term in the flux F , the error in the flux computation must be smaller than $O(\varepsilon^2)$. The error term for F in Theorem 1 is of the form $(\varepsilon/\eta)^{q+2}$. We thus need to choose q and η such that $(\varepsilon/\eta)^{q+2} < \varepsilon^2$, or $\eta > \varepsilon^{1-\alpha}$ with $\alpha = \frac{2}{q+2}$. Recalling that in the finite time case we always take $\eta \sim \varepsilon$, this hence explains why we need to have more accurate kernels or bigger micro boxes in the long time case. We note that in order to maintain a low computational cost we should have α small, which can be obtained by taking a large q , i.e. a very regular kernel.

We have left to discuss the correction to the initial data mentioned in Step 2 in Sect. 2. It is well established in HMM that initial data for the microscopic simulation should be consistent with the macroscopic data, in the sense that the reconstruction of the coarse variables from the microscopic simulation, evaluated at its initial point, should agree with actual macroscopic data at this point. In our setting we consider the macroscopic variables as the local average of the microscopic solution,

$$\bar{u}(t, x) \sim \iint K_\eta(t') K_\eta(x') u^\varepsilon(t+t', x+x') dt' dx'.$$

The given macroscopic data is the polynomial $\tilde{Q}(x)$, which interpolates the macroscopic solution at the initial point. The initial data $Q(x)$ for the microscopic simulation is therefore consistent if it generates a microscopic solution $u^\varepsilon(t, x)$ such that

$$\tilde{Q}(x) = \iint K_\eta(t')K_\eta(x')u^\varepsilon(t', x+x')dt'dx'.$$

Using the tools from the Bloch wave analysis above one can show [9] that

$$\iint K_\eta(t')K_\eta(x')u^\varepsilon(t', x+x')dt'dx' = Q(x) + \varepsilon^2\gamma Q''(x) + \text{h.o.t.}$$

if a sufficiently high order kernel is used. The coefficient γ can be computed analytically in some cases, but in general one needs to find it numerically by probing the dynamics once with the initial data $Q_{\text{probe}}(x) = x^2$ and taking

$$\gamma = 2(\tilde{u}_{\text{probe}}(0, x) - x^2)/\varepsilon^2.$$

For the finite time case it is sufficient to take $Q(x) = \tilde{Q}(x)$, but in the long time case the first correction term of size $O(\varepsilon^2)$ is important to include; recall that the flux must be computed with an accuracy that is better than $O(\varepsilon^2)$. Using $\tilde{Q} - \varepsilon^2\gamma\tilde{Q}''$ rather than \tilde{Q} gives a higher order consistency.

3.5 Stability Analysis of the Macro Scheme for the Long Time Effective Equation

A complicating factor in Sect. 3.4 is the stability of the long time effective equation (11). In fact, (11) is ill-posed since $\beta > 0$. Perturbations in initial data grow without bounds as wave numbers become large. Since our HMM algorithm effectively discretizes (11) one must be concerned about the method's stability. In this section we show that as long as the macroscopic discretization is coarse enough, it is indeed stable.

Even though (11) is ill-posed, it can be used as an effective equation after regularization. Since we are interested in low frequency solutions it should be possible to use a regularized version of (11) where high frequencies are suppressed. The equation could for instance be regularized with a low-pass filter P_{low} applied at the macro level,

$$\tilde{u}_{tt} = P_{\text{low}}(\bar{A}\tilde{u}_{xx} + \beta\varepsilon^2\tilde{u}_{xxxx}),$$

or by adding a small 6th order term,

$$\tilde{u}_{tt} = \bar{A}\tilde{u}_{xx} + \beta\varepsilon^2\tilde{u}_{xxxx} + c\varepsilon^4\tilde{u}_{xxxxx},$$

cf. (10) above. Another regularization technique is to use large time and space grid sizes, which can be seen as a type of low-pass filtering. This is what we do in our

HMM. We show here that this approach is stable when the coarse grid size H satisfies a standard CFL condition and in addition $H \geq C\varepsilon$, for some constant C . This explains why our HMM is stable. Moreover, even with such a coarse grid the macroscopic solution can be computed accurately; In Fig. 5 we show an example of a solution obtained through a direct discretization of (11) on a coarse grid. The solution agrees very well with a direct numerical simulation of the full wave equation.

We now apply standard von Neumann stability analysis [21] to show stability of the macro scheme for periodic solutions,

$$\begin{cases} u_m^{n+1} = 2u_m^n - u_m^{n-1} + \frac{K^2}{24H} \left(-f_{m+3/2}^n + 27f_{m+1/2}^n - 27f_{m-1/2}^n + f_{m-3/2}^n \right), \\ f_m^n = (\bar{A}\partial_x + \beta\varepsilon^2\partial_{xxx})p_m^n(x)|_{x=x_m}, \end{cases} \quad (12)$$

used in the HMM algorithm for the 1D problem and long time. Here we denote u_m^n as the numerical approximation of $u(x_m, t_n) = u(mH, nK)$ and K is the time step and H is the grid size. The scheme (12) is fourth order accurate with respect to K and second order with respect to H . We define the interpolation polynomial $p_{m-1/2}^n$ of degree three over four grid points $u_{m-2}^n, u_{m-1}^n, u_m^n$ and u_{m+1}^n . We assume a uniform grid and write down the polynomial $p_{m-1/2}^n$,

$$p_{m-1/2}^n(x) = c_1 + c_2(x - x_{m-2}) + c_3(x - x_{m-2})(x - x_{m-1}) + c_4(x - x_{m-2})(x - x_{m-1})(x - x_m), \quad (13)$$

where the coefficients c_i are given by

$$\begin{cases} c_1 = u_{m-2}^n, \\ c_2 = \frac{u_{m-1}^n - u_{m-2}^n}{H}, \\ c_3 = \frac{u_m^n - 2u_{m-1}^n + u_{m-2}^n}{2H^2}, \\ c_4 = \frac{u_{m+1}^n - 3u_m^n + 3u_{m-1}^n - u_{m-2}^n}{6H^3}. \end{cases} \quad (14)$$

A numerical scheme is said to be stable if

$$\sum_j (u_j^n)^2 \leq C(T) \sum_j (u_j^0)^2 \quad n = 1, 2, \dots, N, \quad Nk = T,$$

for some constant $C(T)$ independent of n . For the discretization (12) we can show stability if the ratio H/ε is large enough.

Theorem 3. *The finite difference scheme (12) applied on the effective equation (11) with 1-periodic boundary conditions, is stable for K and H satisfying*

$$\frac{\varepsilon}{H} \leq \sqrt{\frac{7\bar{A}}{24\beta}}, \quad (15)$$

and

$$\frac{K}{H} \leq \frac{24}{\sqrt{\bar{A}}} \sqrt{h\left(\frac{24\varepsilon^2\beta}{H^2\bar{A}}\right)}, \quad (16)$$

where

$$h(x) = \begin{cases} \frac{1}{784 - 112x}, & 0 \leq x < \frac{21}{5}, \\ \frac{x^2 - 2x + 1}{128(2(x^2 - x + 1)^{3/2} - 2x^3 + 3x^2 + 3x - 2)}, & \frac{21}{5} \leq x \leq 7. \end{cases}$$

Proof. We plug in the value of interpolation polynomials (13) as replacements for the numerical fluxes $f_{m-1/2}^n$ and $f_{m+1/2}^n$ which depend on $u_{m-2}^n, u_{m-1}^n, u_m^n$ and u_{m+1}^n . By doing so, we see that the finite difference scheme (12) will be of the form

$$\begin{aligned} u_m^{n+1} &= 2u_m^n - u_m^{n-1} \\ &+ c(u_{m+3}^n - 54u_{m+2}^n + 783u_{m+1}^n - 1460u_m^n + 783u_{m-1}^n - 54u_{m-2}^n + u_{m-3}^n) \\ &+ cd(-u_{m+3}^n + 30u_{m+2}^n - 111u_{m+1}^n + 164u_m^n - 111u_{m-1}^n + 30u_{m-2}^n - u_{m-3}^n), \end{aligned} \quad (17)$$

where $c = K^2\bar{A}/(24^2H^2)$ and $d = 24\varepsilon^2\beta/(H^2\bar{A})$. We perform the standard von Neumann stability analysis [21, Sect. 2.2] and replace $u_m^n = g^n \exp(imh\xi)$ in the scheme (17). After dividing with $\exp(imh\xi)$, we get a recurrence relation for g^n of the form,

$$g^{n+1} = (2 + cp(v))g^n - g^{n-1}, \quad (18)$$

where $p(v) = Av^3 + Bv^2 + Cv + D$ is a polynomial in $v = \cos\theta$ ($\theta = h\xi$) and where the coefficients A, B, C and D are affine functions in d ,

$$A = -8d + 8, \quad B = 120d - 216, \quad C = -216d + 1560, \quad D = 104d - 1352.$$

The difference equation (18) is stable if the roots r_1, r_2 of its characteristic polynomial $r^2 - (2 + cp(v))r + 1$ satisfy $|r_j| \leq 1$. It is well known that this happens precisely when $|2 + cp(v)| \leq 2$. Hence, the scheme (17) is stable if and only if $-4 \leq cp(v) \leq 0$. The domain of $p(v)$ is $[-1, 1]$ since $v = \cos\theta$. We now continue the proof to find conditions on c and d such that $-4 \leq cp(v) \leq 0$ is fulfilled for $|v| \leq 1$. We start by observing that,

$$\begin{aligned} p(v) &= 8(v-1)(v-13)(v(1-d) - 13 + d), \\ p'(v) &= 24[(1-d)v^2 + 2(5d-9)v + 65 - 9d], \quad p''(v) = 48(v(1-d) + 5d - 9), \end{aligned} \quad (19)$$

and first consider the condition $p(v) \leq 0$ for $|v| \leq 1$. Since $p(1) = 0$ and $p'(1) = 1352 > 0$ independent of d , we just need to make sure that the root $(13-d)/(1-d) \notin [-1, 1]$. This happens when $0 \leq d \leq 7$, which gives (15). Next, we need to check that $p(v) \geq -4/c$ for $|v| \leq 1$. For this we use the derivatives of $p(v)$ in (19). We start with the interval $0 \leq d \leq 21/5$. This is chosen such that $p'(-1) = 96(21-5d) \geq 0$. Moreover, $p''(-1) = 48(6d-10) \geq 0$ for $d \geq 5/3$ and $p''(1) = 48(4d-8) \leq 0$ for $d \leq 2$. Therefore, recalling that $p'(1) = 1352$, the derivative $p'(v)$ must be positive when $|v| \leq 1$ for the d values considered. A necessary and sufficient condition is then that

$$-\frac{4}{c} \leq p(-1) = -448(7-d) \quad \Rightarrow \quad c \leq \frac{1}{112(7-d)}.$$

This gives the $0 \leq x < 21/5$ part of (16). By the same argument there is a point $v^* \in [-1, 1]$ where $p'(v^*) = 0$ when $21/5 \leq d \leq 7$. By solving $p'(v) = 0$ we obtain

$$v^* = \frac{9-5d}{1-d} - \sqrt{\left(\frac{9-5d}{1-d}\right)^2 + \frac{65-9d}{d-1}}. \quad (20)$$

As we showed above $p(v^*) < 0 = p(1)$. Therefore $p(v^*)$ is a minimum and it suffices to make sure that $p(v^*) \geq -4/c$ for $d \in [21/5, 7]$. Plugging (20) into this inequality gives the $21/5 \leq x \leq 7$ part of (16).

4 Conclusions

We have developed and analyzed numerical methods for multiscale wave equations with oscillatory coefficients. The methods are based on the framework of the heterogeneous multiscale method (HMM) and have substantially lower computational complexity than standard discretization algorithms. Convergence is proven in [10] for finite time approximation in the case of periodic coefficients and for multiple dimensions. The effective equation for long time is different from the finite time homogenized equation. After long time, dispersive effects enter and the method has to capture additional effects on the order of $\mathcal{O}(\varepsilon^2)$ [20]. Numerical experiments show that the new techniques accurately and efficiently captures the macroscopic behavior for both finite and long time. It is emphasized that the HMM approach with just minor modifications accurately captures these dispersive phenomena. We prove that our method is stable if the spatial grid in the macro solver is sufficiently coarse.

References

1. Abdulle, A., E, W.: Finite difference heterogeneous multi-scale method for homogenization problems. *J. Comput. Phys.* **191**(1), 18–39 (2003)

2. Abdulle, A., Grote, M.J.: Finite element heterogeneous multiscale method for the wave equation. Preprint (2010)
3. Bensoussan, A., Lions, J.L., Papanicolaou, G.: Asymptotic Analysis in Periodic Structures. North-Holland Pub. Co. (1978)
4. Cioranescu, D., Donato, P.: An Introduction to Homogenization. No. 17 in Oxford Lecture Series in Mathematics and its Applications. Oxford University Press Inc. (1999)
5. E, W., Engquist, B.: The heterogeneous multiscale methods. *Commun. Math. Sci.* pp. 87–133 (2003)
6. E, W., Engquist, B., Li, X., Ren, W., Vanden-Eijnden, E.: Heterogeneous multiscale methods: A review. *Commun. Comput. Phys.* **2**(3), 367–450 (2007)
7. E, W., Ming, P., Zhang, P.: Analysis of the heterogeneous multiscale method for elliptic homogenization problems. *J. Amer. Math. Soc.* **18**(1), 121–156 (2004)
8. Engquist, B., Holst, H., Runborg, O.: Multiscale methods for the wave equation. In: Sixth International Congress on Industrial Applied Mathematics (ICIAM07) and GAMM Annual Meeting, vol. 7. Wiley (2007)
9. Engquist, B., Holst, H., Runborg, O.: Analysis of HMM for wave propagation problems over long time. Work in progress (2010)
10. Engquist, B., Holst, H., Runborg, O.: Multiscale methods for the wave equation. *Comm. Math. Sci.* **9**(1), 33–56 (2011)
11. Engquist, B., Souganidis, P.E.: Asymptotic and numerical homogenization. *Acta Numer.* **17**, 147–190 (2008)
12. Engquist, B., Tsai, Y.H.: Heterogeneous multiscale methods for stiff ordinary differential equations. *Math. Comp.* **74**(252), 1707–1742 (2005). DOI 10.1017/S0962492902000119
13. Jikov, V.V., Kozlov, S.M., Oleinik, O.A.: Homogenization of Differential Operators and Integral Functions. Springer (1991)
14. Kevrekidis, I.G., Gear, C.W., Hyman, J., Kevekidis, P.G., Runborg, O.: Equation-free, coarse-grained multiscale computation: Enabling microscopic simulators to perform system-level tasks. *Comm. Math. Sci.* pp. 715–762 (2003)
15. Li, X., E, W.: Multiscale modelling of the dynamics of solids at finite temperature. *J. Mech. Phys. Solids* **53**, 1650–1685 (2005)
16. Marchenko, V.A., Khruslov, E.Y.: Homogenization of partial differential equations. *Progress in Mathematical Physics* **46** (2006)
17. Ming, P., Yuen, X.: Numerical methods for multiscale elliptic problems. *J. Comput. Phys.* **214**(1), 421–445 (2005). DOI doi:10.1016/j.jcp.2005.09.024
18. Nguetseng, G.: A general convergence result for a functional related to the theory of homogenization. *SIAM J. Math. Anal.* **20**(3), 608–623 (1989). DOI <http://dx.doi.org/10.1137/0520043>
19. Samaey, G.: Patch dynamics: Macroscopic simulation of multiscale systems. Ph.D. thesis, Katholieke Universiteit Leuven (2006)
20. Santosa, F., Symes, W.W.: A dispersive effective medium for wave propagation in periodic composites. *SIAM J. Appl. Math.* **51**(4), 984–1005 (1991). DOI <http://dx.doi.org/10.1137/0151049>
21. Strikwerda, J.C.: Finite Difference Schemes and Partial Differential Equations (2nd ed.). SIAM (2004)